

The ordinary surface universality class of the three-dimensional $O(N)$ model

Francesco Parisen Toldin *

*Institute for Theoretical Solid State Physics, RWTH Aachen University,
Otto-Blumenthal-Str. 26, 52074 Aachen, Germany and
JARA-FIT and JARA-CSD, 52056 Aachen, Germany*

We study the critical behavior at the ordinary surface universality class of the three-dimensional $O(N)$ model, bounded by a two-dimensional surface. Using high-precision Monte Carlo simulations of an improved lattice model, where the leading bulk scaling correction is suppressed, and finite-size scaling analysis of the fourth cumulant of the surface magnetization, we obtain precise estimates of the scaling dimension of the surface field operator for $N = 2, 3, 4$. We also determine the fixed-point values of two renormalization-group invariant observables, which characterize the finite-size scaling behavior at the ordinary transition.

I. INTRODUCTION

Critical phenomena in the presence of boundaries or, more generally, defects is a rich field of study, which has attracted over the years numerous experimental [1] and theoretical [2–4] studies. A general renormalization-group (RG) analysis shows that a bulk universality class (UC), describing the critical behavior in the thermodynamic limit, generically splits into several boundary UCs, leading to a rich phase diagram [5]. Furthermore, critical exponents and other universal quantities at boundaries differ from the bulk ones [2, 3]. The simplest setup realizing this framework consists in a d -dimensional critical system bounded by a $(d - 1)$ -dimensional surface: different surface UCs can be then realized by tuning surface couplings. Surface UCs are also relevant for the critical Casimir force [6–13]. Despite being a mature subject, boundary critical phenomena has recently received renewed attention. The discovery of unexpected boundary exponents in some quantum spin models has sparked numerous investigations [14–27]. At the same time, recent progresses in conformal field theory have addressed the problem of boundary and defects in conformally-invariant models [28–40]. Closely related to boundary critical phenomena is the research field of the so-called gapless topological states of matter, and in particular their boundary states [41–49].

In this context, recent advancements have challenged the understanding of the bulk-surface phase diagram of the paradigmatic three-dimensional $O(N)$ UC [50], in the presence of a 2D surface. For an isolated 2D surface, the Mermin-Wagner-Hohenberg theorem [51–53] and its generalizations [54, 55] forbid long-range order for $N \geq 2$. While a 2D $O(2)$ model exhibits the Berezinskii-Kosterlitz-Thouless transition, for $N > 2$ the 2D $O(N)$ model is always disordered [50]. These results are expected to hold also for a surface next to a disordered bulk, for in this case one can imagine to integrate out the bulk degrees of freedom, leading to an effective short-ranged $O(N)$ -invariant interaction on the surface [3, 56]. For a critical bulk, and for $N > 2$, the above considerations may suggest that the surface would not host a phase transition, since the topology of the phase diagram does not dictate

it. In contrast with this argument, in Ref. [57] we have shown that the surface of a 3D $O(3)$ model exhibits a *special* transition, separating the *ordinary* phase with the *extraordinary* one [58]. In fact, a recent field-theoretical analysis has pointed out the existence, for a finite range $2 \leq N \leq N_c$, of a new surface UC of the 3D $O(N)$ model, dubbed “extraordinary-log”, where the two-point function of the order parameter decays as a power of a logarithm [59]. Its existence and the logarithmic exponent is determined by some universal RG amplitudes of the so-called *normal* surface UC, which is realized by imposing a boundary symmetry-breaking field. In Ref. [60] we have extracted these amplitudes by means of Monte Carlo (MC) simulations for $N = 2, 3$. A comparison with direct simulations of the extraordinary-log UC reveals a good agreement, thus quantitatively confirming the nontrivial relation between the normal and the extraordinary-log UC. The field-theoretical analysis of the boundary critical behavior has been recently extended to the case of a plane defect in the three-dimensional $O(N)$ model, where it has been shown that the extraordinary-log phase exists for all N [61]. The extraordinary-log UC has been investigated in various settings [22, 62, 63].

While the extraordinary and the special surface UCs in the 3D $O(N)$ model exist for some values of N only, the ordinary UC is always present; it can be generically realized on the surface of a critical $O(N)$ system, without enhancement of the surface interactions. At the ordinary UC, there is only a single relevant surface operator, corresponding to the order parameter, and its two-point function decays quickly, such that the surface susceptibility is finite [2, 3]. A previous MC determination of the ordinary surface critical exponent for $N = 2, 3$ [64] displays a small discrepancy with truncated conformal bootstrap (TCB) results [30]; the latter is, however, affected by a systematic error, whose magnitude is difficult to estimate [30, 40]. For $N = 4$, we are only aware of the MC study of the ordinary UC in Ref. [65].

In this Letter we provide a precise numerical determination of the scaling dimension of the surface field operator Δ_ϕ at the ordinary UC, for $N = 2, 3, 4$. To this end, we employ high-statistics MC simulations of an “improved” model, where the leading scaling corrections are suppressed, and a finite-size scaling (FSS) analysis of a higher-order cumulant of the surface field. Our results will provide a benchmark for future studies, and in particular for the conformal bootstrap approach [66].

* parisentoldin@physik.rwth-aachen.de

TABLE I. Estimates of the value of $\lambda = \lambda^*$ for which the model (1) is improved, for $N = 2, 3, 4$. In the third column we report the value of the coupling constant $\beta = \beta_c$ at the onset of the critical point, for a value of λ within the uncertainty interval of λ^* .

N	λ^*	$(\lambda, \beta_c(\lambda))$
2	2.15(5) [67]	(2.15, 0.508 749 88(6)) [68]
3	5.17(11) [69]	(5.2, 0.687 985 21(8)) [69]
4	18.4(9) [70]	(18.5, 0.917 875 55(17)) [70]

II. MODEL

We study the classical ϕ^4 model on a three-dimensional $L \times L \times L$ lattice, imposing periodic boundary conditions (BC) on two directions, and open BC along the remaining one, thus realizing two surfaces. The reduced Hamiltonian \mathcal{H} , such that the Gibbs weight is $\exp(-\mathcal{H})$, is

$$\mathcal{H} = -\beta \sum_{\langle i j \rangle} \vec{\phi}_i \cdot \vec{\phi}_j - \beta_s \sum_{\langle i j \rangle_s} \vec{\phi}_i \cdot \vec{\phi}_j + \sum_i [\vec{\phi}_i^2 + \lambda(\vec{\phi}_i^2 - 1)^2], \quad (1)$$

where $\vec{\phi}_x$ is an N -components real field on the lattice site x , the first sum extends over the nearest-neighbor pairs where at least one site belongs to the inner bulk, the second sum over the sites on the two surfaces, and the last term is summed over all lattice sites. In the Hamiltonian (1) the coupling constants β and λ determine the bulk behavior, whereas β_s control the surface interactions; here, we consider an identical coupling strength on the two surfaces.

In the limit $\lambda \rightarrow \infty$, the model reduces to the standard hard spin $O(N)$ model. In the (λ, β) plane, the bulk phase diagram exhibits a second-order transition line in the $O(N)$ UC [50, 67, 70, 71]. Along this critical line, for $N \leq 4$ there is a specific point $(\lambda^*, \beta_c(\lambda^*))$ where the model is improved, i.e., the leading scaling correction vanishes. In Table I we report the improvement value λ^* and the corresponding critical coupling $\beta = \beta_c(\lambda)$ for $N = 2, 3, 4$, as determined in previous studies [67–70]. Improved models are a rather useful tool to obtain accurate results in numerical studies of critical phenomena [50], in particular in the presence of boundaries [57, 60, 72–81], whose presence gives rise to additional corrections to scaling, which cumulate with those originating from bulk irrelevant perturbations.

To realize the ordinary UC, we fix β and λ to the values reported in the third column of Table I, thus tuning the bulk to its critical point, and set $\beta_s = \beta$. This choice corresponds to the absence of enhancement of the surface interactions, and generically realizes the ordinary UC; further surface phases and a transition may be explored by tuning the surface interaction strength, while keeping the bulk to its critical point [2, 3]. We numerically sample the model by means of MC simulations, combining Metropolis, overrelaxation, and Wolff single-cluster updates [82]; details of the simulation algorithm are reported in Ref. [57]. To improve the statistics, for every surface observable we perform an average of the values sampled on the two identical surfaces.

III. RESULTS

The scaling dimension of the surface field or, equivalently, of the surface field operator can be computed by a FSS analysis of the correlations of the lattice field ϕ on the surface. To this end, the most commonly used quantity is the surface susceptibility χ_s , defined as

$$\chi_s \equiv \frac{1}{L^2} \langle \vec{M}_s \cdot \vec{M}_s \rangle, \quad \vec{M}_s \equiv \sum_{i \in S} \vec{\phi}_i. \quad (2)$$

where the sum in the definition of the surface magnetization \vec{M}_s extends over the sites on one surface. By a standard FSS analysis [83], at the ordinary critical point and in a finite size χ_s scales as

$$\chi_s = AL^{2-2\Delta_{\hat{\phi}}} + B, \quad (3)$$

where $\Delta_{\hat{\phi}}$ is the scaling dimension of the relevant $O(N)$ -vector operator at the surface, A and B are two nonuniversal constants, and we have neglected scaling corrections. The scaling dimension of the surface operator $\Delta_{\hat{\phi}}$ is related to that of the surface field y_{h_1} by $\Delta_{\hat{\phi}} = 2 - y_{h_1}$, and to the critical exponent η_{\parallel} by $\Delta_{\hat{\phi}} = (1 + \eta_{\parallel})/2$. As is well known, at the ordinary UC χ_s is finite [2, 3], hence the exponent in Eq. (3) $2 - 2\Delta_{\hat{\phi}} < 0$, and the scaling behavior of χ_s is dominated by the nonuniversal background term B . In fact, as shown below, the exponent of the singular part is $2 - 2\Delta_{\hat{\phi}} \approx -0.4$; its smallness exacerbates the FSS analysis of χ_s , because one needs to clearly separate the background term from the slow-decaying singular part $\propto L^{-0.4}$. On top of that, scaling corrections not considered in Eq. (3) further hinder a precise scaling analysis of χ_s , rendering this observable not suitable for a quantitatively accurate determination of $\Delta_{\hat{\phi}}$. To overcome this problem, we have sampled the fourth cumulant χ_{4s} of the surface magnetization. It can be defined by considering an external field \vec{h}_s on a single surface and coupled to the surface magnetization \vec{M}_s , therefore adding to the reduced Hamiltonian (1) a term $-\vec{h}_s \cdot \vec{M}_s$. The fourth cumulant χ_{4s} is then defined as

$$\chi_{4s} \equiv -\frac{1}{L^2} \left. \frac{\partial^4 f}{(\partial \vec{h}_s \cdot \partial \vec{h}_s)^2} \right|_{\vec{h}_s=0}, \quad (4)$$

where $f \equiv -\ln Z$ is the free energy in units of $k_B T$, with Z the partition function; the factor $1/L^2$ in Eq. (4) is due to the fact that \vec{h}_s is applied only on the surface. A straightforward computation of Eq. (4) results in

$$\chi_{4s} = \frac{1}{L^2} \left[\langle (\vec{M}_s \cdot \vec{M}_s)^2 \rangle - \langle \vec{M}_s \cdot \vec{M}_s \rangle^2 - 2 \sum_{i,j=1}^N \langle M_s^{(i)} M_s^{(j)} \rangle \langle M_s^{(i)} M_s^{(j)} \rangle \right], \quad (5)$$

where $M_s^{(i)}$ is the i -th component of \vec{M}_s . The last term in Eq. (5) is nonvanishing only when $i = j$. Furthermore,

with the $O(N)$ symmetry being unbroken, $\langle (M_s^{(i)})^2 \rangle = \langle \vec{M}_s \cdot \vec{M}_s \rangle / N$. Thus, Eq. (5) simplifies to

$$\chi_{4s} = \frac{1}{L^2} \left[\langle (\vec{M}_s \cdot \vec{M}_s)^2 \rangle - \left(\frac{N+2}{N} \right) \langle \vec{M}_s \cdot \vec{M}_s \rangle^2 \right]. \quad (6)$$

The FSS behavior of χ_{4s} at the critical point is

$$\chi_{4s} = AL^{6-4\Delta_\phi} \left(1 + \frac{C}{L} \right) + B, \quad (7)$$

where we have anticipated that the leading scaling correction is $\propto L^{-1}$. Indeed, in the improved lattice model considered here the leading irrelevant bulk scaling field is suppressed, and the next-to-leading correction, due to the lowest nonrotationally invariant irrelevant operator, decays fast as $\propto L^{-\omega_{\text{nr}}}$, with $\omega_{\text{nr}} \simeq 2$ [84]. On the other hand, the surface operator spectrum contains a protected operator, the displacement operator, which encodes the broken translational invariance and whose existence is guaranteed on any conformal defect [31]; its dimension is $\Delta_D = 3$, thus giving rise to corrections to scaling $\propto L^{-1}$. The existence of such corrections was first pointed out in Ref. [85] and can also be intuitively understood by an RG analysis of the scaling field associated with the size L [86]. Although *a priori* the surface operator spectrum may contain more irrelevant perturbations, previous investigations on improved lattice models at the ordinary UC did not detect corrections decaying slower than L^{-1} [72, 75, 78]. The results of this work support this picture, thus we conclude that Eq. (7) reliably describes the leading scaling behavior of χ_{4s} .

To determine Δ_ϕ we have sampled the model (1) by means of high-precision MC simulations, for $N = 2, 3, 4$ and lattice sizes $L = 8, \dots, 384$. As confirmed by fit results below, the leading exponent in Eq. (7) $6-4\Delta_\phi \simeq 1.2 > 0$, so that χ_{4s} diverges and its FSS behavior is, unlike χ , dominated by its singular part. The background term B represents a correction to scaling, effectively decaying as $L^{4\Delta_\phi-6} \sim L^{-1.2}$. As this exponent is rather close to 1, in the FSS analysis it is not technically feasible to reliably disentangle the two equally important sources of corrections CL^{-1} and $BL^{4\Delta_\phi-6}$. Therefore, we resolved to consider separately fits of MC data to Eq. (7) by either fixing $B = 0$ or $C = 0$ [87]. Such a procedure is expected to introduce a small bias in the fitted results, which nevertheless should be negligible for large enough lattice sizes: indeed, on increasing L , scaling corrections become numerically less significant, such that eventually both fits should give identical results. Accordingly, and also in order to monitor residual subleading scaling corrections not considered in Eq. (7), fits are repeated disregarding systematically the smallest lattices. In Fig. 1 we show fitted values of Δ_ϕ , as a function of the minimum lattice size L_{min} taken into account. Fits exhibit a good $\chi^2/\text{d.o.f.}$ (d.o.f. indicates the degrees of freedom) for $L_{\text{min}} \geq 16$ and in some cases also for $L_{\text{min}} = 12$. In line with the discussion above, we observe a small difference in the fitted value of Δ_ϕ as obtained fixing either $B = 0$ or $C = 0$ in Eq. (7). Such a discrepancy is lifted when $L_{\text{min}} = 16$ for $N = 2$ and $L_{\text{min}} = 32$ for $N = 3, 4$. For $N = 2$, on further discarding smaller lattices, we observe a slightly significant drift in the fitted values, hinting at residual scaling corrections:

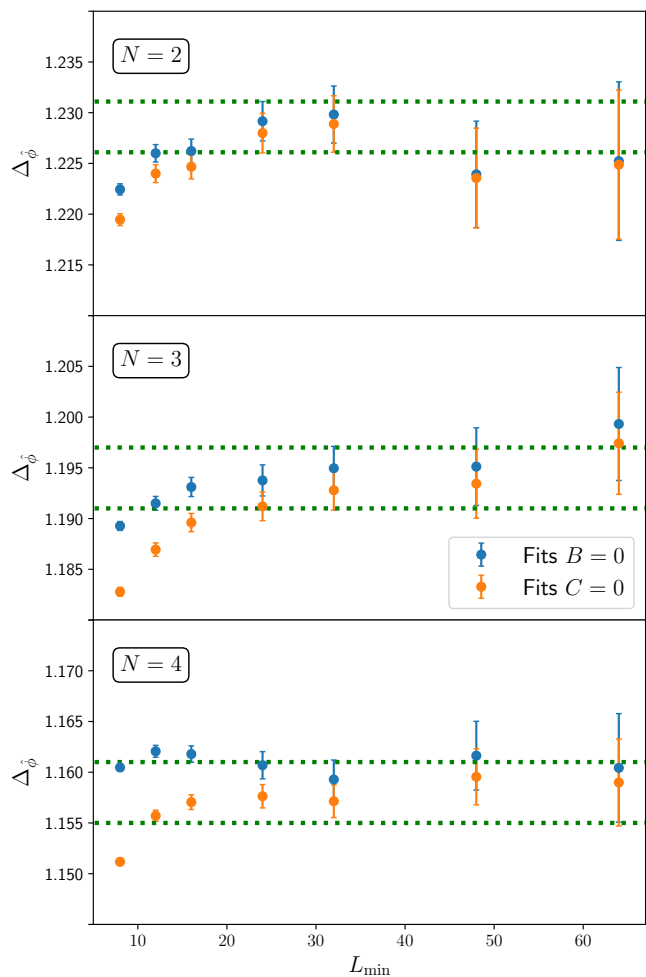


FIG. 1. Fitted value of Δ_ϕ for $N = 2, 3, 4$, and as a function of the minimum lattice size L_{min} taken into account. Results are obtained by fitting χ_{4s} to Eq. (7), and fixing either $B = 0$ or $C = 0$. Dotted lines indicate an interval of one error bar around the final estimates given in Table II.

fits for $L_{\text{min}} = 24, 32$ still give identical results when $B = 0$ or $C = 0$, but the fitted value of Δ_ϕ is in marginal agreement with the results for $L_{\text{min}} = 16$. For this reason, we extract as a final estimate an average of the values obtained in the two fits for $L_{\text{min}} = 24$, indicating a conservative error bar to be fully compatible with both fits; such an estimate also agrees with fit results for $L_{\text{min}} = 16$ within one error bar. For $N = 3, 4$, fits with $L_{\text{min}} \geq 32$ are perfectly stable and give indistinguishable results when setting either $B = 0$ or $C = 0$. Accordingly, we quote as a final estimate of Δ_ϕ an average of the values obtained in the two fits for $L_{\text{min}} = 32$. In Table II we report our results, comparing them with previous determinations present in the literature. We complement our estimate for $N = 4$ by an analysis of the available field-theory series [3, 88–93] and a TCB [94] calculation [87].

Another set of interesting universal quantities at a critical point are the fixed-point values of RG invariants. Here, we consider two such observables: the ratio (Z_a/Z_p) of the par-

TABLE II. Scaling dimension $\Delta_{\hat{\phi}}$ of the leading surface operator at the ordinary transition of the three-dimensional $O(N)$ model. We compare present determinations with results obtained by the field-theoretic ε -expansion setting $\varepsilon = 1$ (ε -exp), the massive field theory approach in $d = 3$ (FT $d = 3$) analyzed with a Padé resummation, TCB, and previous MC simulations. The scaling dimension of the surface field y_{h_1} is related to $\Delta_{\hat{\phi}}$ by $y_{h_1} = 2 - \Delta_{\hat{\phi}}$. The surface critical exponent η_{\parallel} can be expressed in terms of $\Delta_{\hat{\phi}}$ by $\Delta_{\hat{\phi}} = (1 + \eta_{\parallel})/2$ [3].

N	Method	Ref.	$\Delta_{\hat{\phi}}$
2	ε -exp	[3, 88–90]	1.19
	FT $d = 3$	[91, 92]	1.211
	TCB	[30]	1.2342(9)
	MC	[64]	1.219(2)
	MC	This work	1.2286(25)
3	ε -exp	[3, 88–90]	1.153
	FT $d = 3$	[91, 92]	1.169
	TCB	[30]	1.198(1)
	MC	[64]	1.187(2)
	MC	This work	1.194(3)
4	ε -exp	[3, 88–90]	1.125
	FT $d = 3$	This work	1.188
	TCB	This work	1.172
	MC	[65]	0.9798(12)
	MC	This work	1.158(3)

tion function with antiperiodic and periodic BC on a direction parallel to the surfaces, which can be efficiently sampled with the boundary-flip algorithm [95, 96], and the combination $L\Upsilon$, where Υ is helicity modulus, i.e., the response to a torsion on a lateral direction [97]. We notice that other commonly used RG invariants, such as the ratio ξ/L of the surface correlations length ξ over the size L , and the surface Binder cumulant $U_4 = \langle (\vec{M}_s \cdot \vec{M}_s)^2 \rangle / \langle \vec{M}_s \cdot \vec{M}_s \rangle^2$ are not particularly informative here: at the ordinary UC they acquire a trivial fixed-point value $(\xi/L)^* = 0$ and $U_4^* = (N + 2)/N$. We fit RG-invariant observables R to

$$R = R^* (1 + A/L), \quad (8)$$

leaving R^* and A as free parameters. By judging conservatively the variation of the fit results on discarding smallest lattices, and the value of the $\chi^2/\text{d.o.f.}$, we obtain the estimates reported in Table III [87].

IV. DISCUSSION

In this Letter we have studied the ordinary surface UC of the three-dimensional $O(N)$ model, providing an accurate estimate of the scaling dimension $\Delta_{\hat{\phi}}$ of the single relevant surface operator. A comparison with previous MC estimates, reported in Table II, indicates a small, but numerically significant,

deviation from previous results, which are not compatible within one error bar. Particularly significant is the difference between our estimate of $\Delta_{\hat{\phi}}$ for $N = 4$ and the result of Ref. [65]. Here, we have simulated an improved model,

TABLE III. Estimated critical value of RG invariants (Z_a/Z_p) and $L\Upsilon$.

N	$(Z_a/Z_p)^*$	$(L\Upsilon)^*$
2	0.7016(2)	0.175(3)
3	0.56480(8)	0.1819(9)
4	0.44588(9)	0.1866(11)

where leading bulk scaling corrections are suppressed. Furthermore, unlike previous studies which analyzed the surface susceptibility χ , here $\Delta_{\hat{\phi}}$ is extracted by a FSS analysis of the fourth cumulant χ_{4s} ; different than χ , whose scaling behavior is dominated by its nonsingular part, χ_{4s} is divergent [compare Eq. (3) with Eq. (7)]. Hence, we expect our estimates to be more reliable than previous determinations, constituting a benchmark for future studies. In Table II, we also compare our results for $\Delta_{\hat{\phi}}$ with TCB estimates. This method introduces a small systematic error, whose magnitude is difficult to independently estimate [30, 40]. Still, TCB provides a rather good approximation of the boundary exponent, with a deviation of $\lesssim 1\%$ from the MC estimates.

In this work we have also studied the RG invariants at the ordinary transition. These quantities are commonly used in the FSS analysis of second-order phase transitions. In particular, they can be exploited in the scheme of FSS at fixed RG invariant [98], for which in some cases a significant reduction of error bars has been observed [99–102]; a comprehensive review of this method, together with a discussion of its implementation, can be found in Ref. [68]. Within this scheme, our estimates of the fixed-point values of RG invariants reported in Table III provide a base for further numerical improvement of the critical exponents at the ordinary UC.

V. ACKNOWLEDGMENTS

The author is grateful to Hans-Werner Diehl and Marco Meineri for useful communications. F.P.T. is funded by the Deutsche Forschungsgemeinschaft (DFG, German Research Foundation), Project No. 414456783. The author gratefully acknowledges the Gauss Centre for Supercomputing e.V. (www.gauss-centre.eu) for funding this project by providing computing time through the John von Neumann Institute for Computing (NIC) on the GCS Supercomputer JUWELS at Jülich Supercomputing Centre (JSC). The author acknowledges support from the University of Würzburg, where this work was initiated.

[1] H. Dosch, *Critical Phenomena at Surfaces and Interfaces: Evanescent X-Ray and Neutron Scattering*, Springer Tracts in

Modern Physics (Springer Berlin Heidelberg, Berlin, 2006).

- [2] K. Binder, Critical behavior at surfaces, in *Phase Transitions and Critical Phenomena*, Vol. 8, edited by C. Domb and J. L. Lebowitz (Academic Press, London, 1983) p. 1.
- [3] H. W. Diehl, Field-theoretical approach to critical behaviour at surfaces, in *Phase Transitions and Critical Phenomena*, Vol. 10, edited by C. Domb and J. L. Lebowitz (Academic Press, London, 1986) p. 75.
- [4] M. Pleimling, Critical phenomena at perfect and non-perfect surfaces, *J. Phys. A: Math. Gen.* **37**, R79 (2004), [cond-mat/0402574](#).
- [5] J. Cardy, *Scaling and Renormalization in Statistical Physics* (Cambridge University Press, Cambridge, 1996).
- [6] M. E. Fisher and P.-G. de Gennes, Phénomènes aux parois dans un mélange binaire critique, *C. R. Acad. Sci. Paris Ser. B* **287**, 207 (1978).
- [7] M. Krech, *The Casimir Effect in Critical Systems* (World Scientific, London, 1994).
- [8] M. Krech, Fluctuation-induced forces in critical fluids, *J. Phys.: Condens. Matter* **11**, R391 (1999), [cond-mat/9909413](#).
- [9] J. G. Brankov, D. M. Danchev, and N. S. Tonchev, *Theory of Critical Phenomena in Finite-size Systems: Scaling and Quantum Effects*, Series in modern condensed matter physics (World Scientific, Singapore, 2000).
- [10] A. Gambassi, The Casimir effect: From quantum to critical fluctuations, *J. Phys.: Conf. Ser.* **161**, 012037 (2009), [arXiv:0812.0935 \[cond-mat.stat-mech\]](#).
- [11] A. Gambassi and S. Dietrich, Critical Casimir forces steered by patterned substrates, *Soft Matter* **7**, 1247 (2011), [arXiv:1011.1831 \[cond-mat.soft\]](#).
- [12] A. Maciołek and S. Dietrich, Collective behavior of colloids due to critical Casimir interactions, *Rev. Mod. Phys.* **90**, 045001 (2018), [arXiv:1712.06678 \[cond-mat.soft\]](#).
- [13] D. M. Dantchev and S. Dietrich, Critical Casimir effect: Exact results, *Phys. Rep.* **1005**, 1 (2023), [arXiv:2203.15050 \[cond-mat.stat-mech\]](#).
- [14] T. Suzuki and M. Sato, Gapless edge states and their stability in two-dimensional quantum magnets, *Phys. Rev. B* **86**, 224411 (2012), [arXiv:1209.3097 \[cond-mat.str-el\]](#).
- [15] L. Zhang and F. Wang, Unconventional Surface Critical Behavior Induced by a Quantum Phase Transition from the Two-Dimensional Affleck-Kennedy-Lieb-Tasaki Phase to a Néel-Ordered Phase, *Phys. Rev. Lett.* **118**, 087201 (2017), [arXiv:1611.06477 \[cond-mat.str-el\]](#).
- [16] C. Ding, L. Zhang, and W. Guo, Engineering Surface Critical Behavior of $(2 + 1)$ -Dimensional $O(3)$ Quantum Critical Points, *Phys. Rev. Lett.* **120**, 235701 (2018), [arXiv:1801.10035 \[cond-mat.str-el\]](#).
- [17] L. Weber, F. Parisen Toldin, and S. Wessel, Nonordinary edge criticality of two-dimensional quantum critical magnets, *Phys. Rev. B* **98**, 140403(R) (2018), [arXiv:1804.06820 \[cond-mat.str-el\]](#).
- [18] L. Weber and S. Wessel, Nonordinary criticality at the edges of planar spin-1 heisenberg antiferromagnets, *Phys. Rev. B* **100**, 054437 (2019), [arXiv:1906.07051 \[cond-mat.str-el\]](#).
- [19] C.-M. Jian, Y. Xu, X.-C. Wu, and C. Xu, Continuous Néel-VBS quantum phase transition in non-local one-dimensional systems with $SO(3)$ symmetry, *SciPost Phys.* **10**, 033 (2021), [arXiv:2004.07852 \[cond-mat.str-el\]](#).
- [20] W. Zhu, C. Ding, L. Zhang, and W. Guo, Surface critical behavior of coupled Haldane chains, *Phys. Rev. B* **103**, 024412 (2021), [arXiv:2010.10920 \[cond-mat.str-el\]](#).
- [21] L. Weber and S. Wessel, Spin versus bond correlations along dangling edges of quantum critical magnets, *Phys. Rev. B* **103**, L020406 (2021), [arXiv:2010.15691 \[cond-mat.str-el\]](#).
- [22] C. Ding, W. Zhu, W. Guo, and L. Zhang, Special Transition and Extraordinary Phase on the Surface of a $(2+1)$ -Dimensional Quantum Heisenberg Antiferromagnet, [arXiv:2110.04762 \(2021\)](#), [arXiv:2110.04762 \[cond-mat.str-el\]](#).
- [23] Z. Wang, F. Zhang, and W. Guo, Bulk and surface critical behavior of a quantum Heisenberg antiferromagnet on two-dimensional coupled diagonal ladders, *Phys. Rev. B* **106**, 134407 (2022), [arXiv:2207.05248 \[cond-mat.str-el\]](#).
- [24] Y. Sun, J. Lyu, and J.-P. Lv, Classical-quantum correspondence of special and extraordinary-log criticality: Villain's bridge, *Phys. Rev. B* **106**, 174516 (2022), [arXiv:2211.11376 \[cond-mat.stat-mech\]](#).
- [25] X.-J. Yu, R.-Z. Huang, H.-H. Song, L. Xu, C. Ding, and L. Zhang, Conformal Boundary Conditions of Symmetry-Enriched Quantum Critical Spin Chains, *Phys. Rev. Lett.* **129**, 210601 (2022), [arXiv:2111.10945 \[cond-mat.str-el\]](#).
- [26] Y. Sun and J.-P. Lv, Quantum extraordinary-log universality of boundary critical behavior, *Phys. Rev. B* **106**, 224502 (2022), [arXiv:2205.00878 \[cond-mat.stat-mech\]](#).
- [27] Y. Xu, C. Peng, Z. Xiong, and L. Zhang, Persistent corner spin mode at the quantum critical point of a plaquette Heisenberg model, *Phys. Rev. B* **106**, 214409 (2022), [arXiv:2112.04616 \[cond-mat.str-el\]](#).
- [28] D. M. McAvity and H. Osborn, Conformal field theories near a boundary in general dimensions, *Nucl. Phys. B* **455**, 522 (1995), [arXiv:cond-mat/9505127 \[cond-mat\]](#).
- [29] P. Liendo, L. Rastelli, and B. C. van Rees, The bootstrap program for boundary CFT_d , *J. High Energy Phys.* **2013**, 113 (2013), [arXiv:1210.4258 \[hep-th\]](#).
- [30] F. Gliozzi, P. Liendo, M. Meineri, and A. Rago, Boundary and interface CFTs from the conformal bootstrap, *J. High Energy Phys.* **2015**, 36 (2015), [arXiv:1502.07217 \[hep-th\]](#).
- [31] M. Billò, V. Gonçalves, E. Lauria, and M. Meineri, Defects in conformal field theory, *J. High Energy Phys.* **2016**, 91 (2016), [arXiv:1601.02883 \[hep-th\]](#).
- [32] P. Liendo and C. Meneghelli, Bootstrap equations for $N = 4$ SYM with defects, *J. High Energy Phys.* **2017**, 122 (2017), [arXiv:1608.05126 \[hep-th\]](#).
- [33] E. Lauria, M. Meineri, and E. Trevisani, Radial coordinates for defect CFTs, *J. High Energy Phys.* **2018**, 148 (2018), [arXiv:1712.07668 \[hep-th\]](#).
- [34] D. Mazáč, L. Rastelli, and X. Zhou, An analytic approach to $BCFT_d$, *J. High Energy Phys.* **2019**, 4 (2019), [arXiv:1812.09314 \[hep-th\]](#).
- [35] A. Kaviraj and M. F. Paulos, The Functional Bootstrap for Boundary CFT, *J. High Energy Phys.* **4**, arXiv:1812.04034 (2020), [arXiv:1812.04034 \[hep-th\]](#).
- [36] P. Dey, T. Hansen, and M. Shpot, Operator expansions, layer susceptibility and two-point functions in $BCFT$, *J. High Energy Phys.* **2020**, 51 (2020), [arXiv:2006.11253 \[hep-th\]](#).
- [37] C. Behan, L. Di Pietro, E. Lauria, and B. C. van Rees, Bootstrapping boundary-localized interactions, *J. High Energy Phys.* **2020**, 182 (2020), [arXiv:2009.03336 \[hep-th\]](#).
- [38] A. Gimenez-Grau, P. Liendo, and P. van Vliet, Superconformal boundaries in $4 - \epsilon$ dimensions, *J. High Energy Phys.* **2021**, 167 (2021), [arXiv:2012.00018 \[hep-th\]](#).
- [39] N. Andrei, A. Bissi, M. Buican, J. Cardy, P. Dorey, N. Drukker, J. Erdmenger, D. Friedan, D. Fursaev, A. Konechny, C. Kristjansen, I. Makabe, Y. Nakayama, A. O'Bannon, R. Parini, B. Robinson, S. Ryu, C. Schmidt-Colinet, V. Schomerus, C. Schweigert, and G. M. T. Watts, Boundary and defect CFT: open problems and applications,

- J. Phys. A: Math. Theor.* **53**, 453002 (2020).
- [40] J. Padayasi, A. Krishnan, M. A. Metlitski, I. A. Gruzberg, and M. Meineri, The extraordinary boundary transition in the 3d $O(N)$ model via conformal bootstrap, *SciPost Physics* **12**, arXiv:2111.03071 (2022), arXiv:2111.03071 [cond-mat.stat-mech].
- [41] T. Grover and A. Vishwanath, Quantum Criticality in Topological Insulators and Superconductors: Emergence of Strongly Coupled Majoranas and Supersymmetry, arXiv:1206.1332 (2012), arXiv:1206.1332 [cond-mat.str-el].
- [42] M. Barkeshli and X.-L. Qi, Synthetic Topological Qubits in Conventional Bilayer Quantum Hall Systems, *Phys. Rev. X* **4**, 041035 (2014), arXiv:1302.2673 [cond-mat.mes-hall].
- [43] J. Cano, M. Cheng, M. Barkeshli, D. J. Clarke, and C. Nayak, Chirality-protected Majorana zero modes at the gapless edge of Abelian quantum Hall states, *Phys. Rev. B* **92**, 195152 (2015), arXiv:1505.07825 [cond-mat.str-el].
- [44] M. Barkeshli, M. Mulligan, and M. P. A. Fisher, Particle-hole symmetry and the composite Fermi liquid, *Phys. Rev. B* **92**, 165125 (2015), arXiv:1502.05404 [cond-mat.str-el].
- [45] T. Scaffidi, D. E. Parker, and R. Vasseur, Gapless Symmetry-Protected Topological Order, *Phys. Rev. X* **7**, 041048 (2017), arXiv:1705.01557 [cond-mat.str-el].
- [46] D. E. Parker, T. Scaffidi, and R. Vasseur, Topological luttinger liquids from decorated domain walls, *Phys. Rev. B* **97**, 165114 (2018), arXiv:1711.09106 [cond-mat.str-el].
- [47] R. Verresen, Topology and edge states survive quantum criticality between topological insulators, arXiv:2003.05453 (2020), arXiv:2003.05453 [cond-mat.str-el].
- [48] R. Verresen, R. Thorngren, N. G. Jones, and F. Pollmann, Gapless Topological Phases and Symmetry-Enriched Quantum Criticality, *Phys. Rev. X* **11**, 041059 (2021), arXiv:1905.06969 [cond-mat.str-el].
- [49] R. Thorngren, A. Vishwanath, and R. Verresen, Intrinsically gapless topological phases, *Phys. Rev. B* **104**, 075132 (2021), arXiv:2008.06638 [cond-mat.str-el].
- [50] A. Pelissetto and E. Vicari, Critical phenomena and renormalization-group theory, *Phys. Rep.* **368**, 549 (2002), cond-mat/0012164.
- [51] N. D. Mermin and H. Wagner, Absence of Ferromagnetism or Antiferromagnetism in One- or Two-Dimensional Isotropic Heisenberg Models, *Phys. Rev. Lett.* **17**, 1133 (1966); Erratum: Absence of Ferromagnetism or Antiferromagnetism in One- or Two-Dimensional Isotropic Heisenberg Models, *Phys. Rev. Lett.* **17**, 1307 (1966).
- [52] P. C. Hohenberg, Existence of Long-Range Order in One and Two Dimensions, *Phys. Rev.* **158**, 383 (1967).
- [53] B. I. Halperin, On the Hohenberg-Mermin-Wagner Theorem and Its Limitations, *J. Stat. Phys.* **175**, 521 (2019), arXiv:1812.00220 [cond-mat.stat-mech].
- [54] D. Cassi, Phase transitions and random walks on graphs: A generalization of the Mermin-Wagner theorem to disordered lattices, fractals, and other discrete structures, *Phys. Rev. Lett.* **68**, 3631 (1992).
- [55] F. Merkl and H. Wagner, Recurrent random walks and the absence of continuous symmetry breaking on graphs, *J. Stat. Phys.* **75**, 153 (1994).
- [56] We thank H. W. Diehl for this argument.
- [57] F. Parisen Toldin, Boundary critical behavior of the three-dimensional Heisenberg universality class, *Phys. Rev. Lett.* **126**, 135701 (2021), arXiv:2012.00039 [cond-mat.stat-mech].
- [58] Earlier hint of surface transition were found in Ref. [64].
- [59] M. A. Metlitski, Boundary criticality of the $O(N)$ model in $d = 3$ critically revisited, *SciPost Phys.* **12**, 131 (2022), arXiv:2009.05119 [cond-mat.str-el].
- [60] F. Parisen Toldin and M. A. Metlitski, Boundary criticality of the 3d $O(N)$ model: from normal to extraordinary, *Phys. Rev. Lett.* **128**, arXiv:2111.03613 (2022), arXiv:2111.03613 [cond-mat.stat-mech].
- [61] A. Krishnan and M. A. Metlitski, A plane defect in the 3d $O(N)$ model, arXiv:2301.05728 (2023) [cond-mat.str-el].
- [62] M. Hu, Y. Deng, and J.-P. Lv, Extraordinary-Log Surface Phase Transition in the Three-Dimensional X Y Model, *Phys. Rev. Lett.* **127**, 120603 (2021), arXiv:2104.05152 [cond-mat.stat-mech].
- [63] Y. Sun, M. Hu, and J.-P. Lv, Extraordinary-log Universality of Critical Phenomena in Plane Defects, arXiv:2301.11720 (2023) [cond-mat.stat-mech].
- [64] Y. Deng, H. W. J. Blöte, and M. P. Nightingale, Surface and bulk transitions in three-dimensional $O(n)$ models, *Phys. Rev. E* **72**, 016128 (2005), cond-mat/0504173.
- [65] Y. Deng, Bulk and surface phase transitions in the three-dimensional $O(4)$ spin model, *Phys. Rev. E* **73**, 056116 (2006).
- [66] D. Poland, S. Rychkov, and A. Vichi, The conformal bootstrap: Theory, numerical techniques, and applications, *Rev. Mod. Phys.* **91**, 015002 (2019), arXiv:1805.04405 [hep-th].
- [67] M. Campostrini, M. Hasenbusch, A. Pelissetto, and E. Vicari, Theoretical estimates of the critical exponents of the superfluid transition in ^4He by lattice methods, *Phys. Rev. B* **74**, 144506 (2006), cond-mat/0605083.
- [68] F. Parisen Toldin, Finite-Size Scaling at fixed Renormalization-Group invariant, *Phys. Rev. E* **105**, 034137, arXiv:2112.00392 [cond-mat.stat-mech].
- [69] M. Hasenbusch, Monte carlo study of a generalized icosahedral model on the simple cubic lattice, *Phys. Rev. B* **102**, 024406 (2020), arXiv:2005.04448 [cond-mat.stat-mech].
- [70] M. Hasenbusch, Three-dimensional $O(N)$ -invariant ϕ^4 models at criticality for $N \geq 4$, *Phys. Rev. B* **105**, 054428 (2022), arXiv:2112.03783 [hep-lat].
- [71] M. Campostrini, M. Hasenbusch, A. Pelissetto, P. Rossi, and E. Vicari, Critical exponents and equation of state of the three-dimensional Heisenberg universality class, *Phys. Rev. B* **65**, 144520 (2002), cond-mat/0110336.
- [72] M. Hasenbusch, The thermodynamic Casimir effect in the neighbourhood of the λ -transition: a Monte Carlo study of an improved three-dimensional lattice model, *J. Stat. Mech.* **P07031**, (2009), arXiv:0905.2096 [cond-mat.stat-mech].
- [73] M. Hasenbusch, Thermodynamic Casimir effect for films in the three-dimensional Ising universality class: Symmetry-breaking boundary conditions, *Phys. Rev. B* **82**, 104425 (2010), arXiv:1005.4749 [cond-mat.stat-mech].
- [74] F. Parisen Toldin and S. Dietrich, Critical Casimir forces and adsorption profiles in the presence of a chemically structured substrate, *J. Stat. Mech.* **P11003**, (2010), arXiv:1007.3913 [cond-mat.stat-mech].
- [75] M. Hasenbusch, Thermodynamic Casimir force: A Monte Carlo study of the crossover between the ordinary and the normal surface universality class, *Phys. Rev. B* **83**, 134425 (2011), arXiv:1012.4986 [cond-mat.stat-mech].
- [76] M. Hasenbusch, Monte Carlo study of surface critical phenomena: The special point, *Phys. Rev. B* **84**, 134405 (2011), arXiv:1108.2425 [cond-mat.stat-mech].
- [77] M. Hasenbusch, Thermodynamic Casimir effect: Universality and corrections to scaling, *Phys. Rev. B* **85**, 174421 (2012), arXiv:1202.6206 [cond-mat.stat-mech].
- [78] F. Parisen Toldin, M. Tröndle, and S. Dietrich, Critical Casimir forces between homogeneous and chemically striped surfaces,

- Phys. Rev. E **88**, 052110 (2013), arXiv:1303.6104 [cond-mat.stat-mech].
- [79] F. Parisen Toldin, Critical Casimir force in the presence of random local adsorption preference, *Phys. Rev. E* **91**, 032105 (2015), arXiv:1308.5220 [cond-mat.stat-mech].
- [80] F. Parisen Toldin, M. Tröndle, and S. Dietrich, Line contribution to the critical Casimir force between a homogeneous and a chemically stepped surface, *J. Phys.: Condens. Matter* **27**, 214010 (2015), arXiv:1409.5536 [cond-mat.stat-mech].
- [81] F. Parisen Toldin, F. F. Assaad, and S. Wessel, Critical behavior in the presence of an order-parameter pinning field, *Phys. Rev. B* **95**, 014401 (2017), arXiv:1607.04270 [cond-mat.stat-mech].
- [82] U. Wolff, Collective Monte Carlo updating for spin systems, *Phys. Rev. Lett.* **62**, 361 (1989).
- [83] V. Privman, Finite-Size Scaling Theory, in *Finite Size Scaling and Numerical Simulation of Statistical Systems*, edited by V. Privman (World Scientific, Singapore, 1990) p. 1.
- [84] M. Campostrini, A. Pelissetto, P. Rossi, and E. Vicari, Two-point correlation function of three-dimensional O(N) models: The critical limit and anisotropy, *Phys. Rev. E* **57**, 184 (1998), cond-mat/9705086.
- [85] T. W. Capehart and M. E. Fisher, Susceptibility scaling functions for ferromagnetic Ising films, *Phys. Rev. B* **13**, 5021 (1976).
- [86] M. Campostrini, A. Pelissetto, and E. Vicari, Finite-size scaling at quantum transitions, *Phys. Rev. B* **89**, 094516 (2014), arXiv:1401.0788 [cond-mat.stat-mech].
- [87] See Supplemental Material for the table of fits of χ_{4s} , a Padé resummation of the massive field-theory expansion of Δ_{ϕ}^{ζ} for $N = 4$, a truncated conformal bootstrap calculation of Δ_{ϕ}^{ζ} for $N = 4$, and details on the analysis of RG-invariant observables.
- [88] J. S. Reeve and A. J. Guttmann, Critical Behavior of the n-Vector Model with a Free Surface, *Phys. Rev. Lett.* **45**, 1581 (1980).
- [89] J. Reeve and A. J. Guttmann, Renormalisation group calculations of the critical exponents of the n-vector model with a free surface, *J. Phys. A: Math. Gen.* **14**, 3357 (1981).
- [90] H. W. Diehl and S. Dietrich, Field-theoretical approach to static critical phenomena in semi-infinite systems, *Z. Phys. B* **42**, 65 (1981); Erratum: Field-theoretical approach to static critical phenomena in semi-infinite systems, *Z. Phys. B* **43**, 281 (1981).
- [91] H. W. Diehl and M. Shpot, Surface critical behavior in fixed dimensions $d < 4$: Nonanalyticity of critical surface enhancement and massive field theory approach, *Phys. Rev. Lett.* **73**, 3431 (1994), arXiv:cond-mat/9409064 [cond-mat].
- [92] H. W. Diehl and M. Shpot, Massive field-theory approach to surface critical behavior in three-dimensional systems, *Nucl. Phys. B* **528**, 595 (1998), arXiv:cond-mat/9804083 [cond-mat.stat-mech].
- [93] S. A. Antonenko and A. I. Sokolov, Critical exponents for a three-dimensional O(n)-symmetric model with $n > 3$, *Phys. Rev. E* **51**, 1894 (1995), hep-th/9803264.
- [94] F. Gliozzi, Constraints on Conformal Field Theories in Diverse Dimensions from the Bootstrap Mechanism, *Phys. Rev. Lett.* **111**, 161602 (2013), arXiv:1307.3111 [hep-th].
- [95] M. Hasenbusch, Monte Carlo simulation with fluctuating boundary conditions, *Physica A* **197**, 423 (1993).
- [96] M. Campostrini, M. Hasenbusch, A. Pelissetto, P. Rossi, and E. Vicari, Critical behavior of the three-dimensional xy universality class, *Phys. Rev. B* **63**, 214503 (2001), arXiv:cond-mat/0010360 [cond-mat.stat-mech].
- [97] M. E. Fisher, M. N. Barber, and D. Jasnow, Helicity modulus, superfluidity, and scaling in isotropic systems, *Phys. Rev. A* **8**, 1111 (1973).
- [98] M. Hasenbusch, A Monte Carlo study of leading order scaling corrections of ϕ^4 theory on a three-dimensional lattice, *J. Phys. A: Math. Gen.* **32**, 4851 (1999), hep-lat/9902026.
- [99] M. Hasenbusch, A. Pelissetto, and E. Vicari, Instability of O(5) multicritical behavior in SO(5) theory of high- T_c superconductors, *Phys. Rev. B* **72**, 014532 (2005), cond-mat/0502327.
- [100] M. Hasenbusch, F. Parisen Toldin, A. Pelissetto, and E. Vicari, The universality class of 3D site-diluted and bond-diluted Ising systems, *J. Stat. Mech.* **P02016**, (2007), cond-mat/0611707.
- [101] U. Wolff, Precision check on the triviality of the ϕ^4 theory by a new simulation method, *Phys. Rev. D* **79**, 105002 (2009), arXiv:0902.3100 [hep-lat].
- [102] F. Parisen Toldin, Improvement of Monte Carlo estimates with covariance-optimized finite-size scaling at fixed phenomenological coupling, *Phys. Rev. E* **84**, 025703(R) (2011), arXiv:1104.2500 [cond-mat.stat-mech].

Supplemental Material

VI. FITS OF THE FOURTH CUMULANT χ_{4s}

In Table S.I we report results of fits of χ_{4s} to Eq. (7), as a function of the minimum lattice size L_{\min} taken into account.

VII. PADÉ RESUMMATION OF MASSIVE FIELD-THEORY RESULTS FOR $N = 4$

In this section we provide details of the analysis of the two-loop expansion of the boundary exponent η_{\parallel} at the ordinary transition for $N = 4$, obtained within the massive field-theory scheme at $d = 3$. Refs. [91, 92] reports the following series expansion at two loops

$$\eta_{\parallel} = 2 - \frac{N+2}{2(N+8)}\bar{u} - \frac{24(N+2)}{(N+8)^2} \left(C + \frac{N+14}{96} \right) \bar{u}^2 + O(\bar{u}^3), \quad C = -0.105063, \quad (\text{S.1})$$

where \bar{u} is a rescaled renormalized coupling constant, such that the β -function is $\beta(\bar{u}) = \bar{u} - \bar{u}^2 + O(\bar{u}^3)$. The knowledge of the surface exponent η_{\parallel} allows to determine the scaling dimension of the surface field by means of a standard scaling relation [3]

$$\Delta_{\hat{\phi}} = \frac{1 + \eta_{\parallel}}{2}. \quad (\text{S.2})$$

In Ref. [92], the series is analyzed for $N = 0, 1, 2, 3$ using a Padé resummation; in particular, the diagonal [1/1] Padé approximant is argued to provide the best result. In order to have a homogeneous comparison, also the value reported in Table II for $N = 4$ has been obtained with the [1/1] Padé approximant of Eq. (S.1). To carry out the calculation, we have used the fixed-point value of $\bar{u}^* = 1.369$ obtained in Ref. [93] with a Padé-Borel resummation of the six-loop expansion of $\beta(\bar{u})$.

VIII. CONFORMAL BOOTSTRAP DETERMINATION OF $\Delta_{\hat{\phi}}$ FOR $N = 4$

In this section we use the truncated conformal bootstrap method [94] to compute the scaling dimension of the boundary field at the ordinary fixed point for $N = 4$. We recall in the following the essential ingredients of the method, following closely Ref. [30], which applied the technique to investigate the boundary exponents of the $O(N)$ model, for $N \leq 3$. We consider a three-dimensional conformal field theory in a semiinfinite space, where we introduce cartesian coordinates $x = (\mathbf{x}, z)$, such that the the boundary surface is located at $z = 0$. We indicate bulk operators by O and boundary ones by \hat{O} , and their corresponding scaling dimensions Δ_O and $\Delta_{\hat{O}}$. Bulk primary operators satisfy an Operator Product Ex-

pansion (OPE)

$$O_1(x)O_2(y) = \frac{\delta_{12}}{(x-y)^{2\Delta_{O_1}}} + \sum_k \lambda_{12k} C(x-y, \partial_y) O_k(y), \quad (\text{S.3})$$

where conformal invariance fixes the form of $C(x-y, \partial_y)$ and λ_{12k} are the OPE coefficients. A boundary OPE holds for $z \rightarrow 0$:

$$O_1(x) = \frac{a_1}{(2z)^{\Delta_{O_1}}} + \sum_l \mu_{1l} D(z, \partial_z) \hat{O}_l(\mathbf{x}), \quad (\text{S.4})$$

where $D(z, \partial_z)$ is fixed by conformal invariance, and μ_{1l} are universal boundary OPE coefficients. A crossing equation for the correlators $\langle O_1(x)O_2(y) \rangle$ can be written employing either Eq. (S.3) or Eq. (S.4). Introducing a Taylor expansion of the crossing equation, and truncating the OPE to n_{bulk} bulk and n_{bdy} boundary operators, one obtains [30]

$$-\sum_{k=1}^{n_{\text{bulk}}} p_k f_{\text{bulk}}^k |_{\xi=1} + \sum_{l=1}^{n_{\text{bdy}}} q_l f_{\text{bdy}}^l |_{\xi=1} + a_1 a_2 = \delta_{12} \quad (\text{S.5})$$

$$-\sum_{k=1}^{n_{\text{bulk}}} p_k \partial_{\xi}^n f_{\text{bulk}}^k |_{\xi=1} + \sum_{l=1}^{n_{\text{bdy}}} q_l \partial_{\xi}^n \left[\xi^{(\Delta_{O_1} + \Delta_{O_2})/2} f_{\text{bdy}}^l \right] |_{\xi=1} + a_1 a_2 \partial_{\xi}^n \xi^{(\Delta_{O_1} + \Delta_{O_2})/2} |_{\xi=1} = 0, \quad n = 1, \dots, M, \quad (\text{S.6})$$

where M is a truncation parameter, $p_k = \lambda_{12k} a_k$, $q_l = \mu_{1l} \mu_{2l}$, and $f_{\text{bulk}}^k, f_{\text{bdy}}^l$ are the bulk and boundary conformal blocks; in $d = 3$ they are [28]

$$f_{\text{bulk}}^k = \xi^{\Delta_{O_k}/2}, \quad 2F_1 \left(\frac{\Delta_{O_k} + \Delta_{12}}{2}, \frac{\Delta_{O_k} - \Delta_{12}}{2}, \Delta_{O_k} - \frac{1}{2}, -\xi \right), \quad \Delta_{12} \equiv \Delta_{O_1} - \Delta_{O_2}, \quad (\text{S.7})$$

$$f_{\text{bdy}}^l = \frac{1}{2\sqrt{\xi}} \left(\frac{4}{1+\xi} \right)^{\Delta_{\hat{O}_l} - 1/2} \left(1 + \sqrt{\frac{\xi}{1+\xi}} \right)^{-2(\Delta_{\hat{O}_l} - 1)}. \quad (\text{S.8})$$

As in Ref. [30], we set in Eqs. (S.5)-(S.6) $O_1 = O_2 = \phi$ the leading $O(4)$ vector, i.e., the order parameter and we truncate the OPE $\phi \times \phi$ [Eq. (S.3)] to the leading $n_{\text{bulk}} = 2$ bulk scalars appearing on the right-hand side of Eq. (S.3): the energy operator ϵ and the leading irrelevant scalar operator ϵ' . The leading operator appearing in the boundary OPE of ϕ is the leading surface vector $\hat{\phi}$. We truncate the right-hand side of Eq. (S.4) to $n_{\text{bdy}} = 1$ boundary operators, i.e., to $\hat{\phi}$, whose scaling dimension $\Delta_{\hat{\phi}}$ is the main target of the computation. As input parameters for the computation, we use the dimensions $\Delta_{\epsilon}, \Delta_{\epsilon'}$ and $\Delta_{\hat{\phi}}$. They are related to the usual exponents

TABLE S.I. Fits of the fourth cumulant χ_{4s} to Eq. (7), for $N = 2, 3, 4$, and as a function of the minimum lattice size L_{\min} taken into account. Fit results are obtained fixing either $B = 0$ or $C = 0$.

N	L_{\min}	Fits $B = 0$		Fits $C = 0$	
		$\Delta_{\hat{\phi}}$	$\chi^2/\text{d.o.f.}$	$\Delta_{\hat{\phi}}$	$\chi^2/\text{d.o.f.}$
2	8	1.22244(55)	3.9	1.21946(58)	6.2
	12	1.22600(86)	0.8	1.22400(89)	1.0
	16	1.2262(12)	0.9	1.2247(12)	1.0
	24	1.2292(19)	0.4	1.2280(19)	0.4
	32	1.2298(28)	0.5	1.2289(28)	0.5
	48	1.2239(52)	0.1	1.2236(49)	0.1
	64	1.2252(78)	0.2	1.2249(74)	0.2
3	8	1.18927(43)	3.1	1.18278(44)	11.1
	12	1.19150(68)	1.2	1.18694(66)	3.3
	16	1.19311(94)	0.5	1.18960(90)	0.9
	24	1.1938(15)	0.6	1.1912(14)	0.7
	32	1.1950(22)	0.5	1.1928(20)	0.6
	48	1.1951(38)	0.7	1.1934(34)	0.7
	64	1.1993(56)	0.6	1.1974(50)	0.6
4	8	1.16047(37)	1.7	1.15117(36)	15.3
	12	1.16206(59)	0.5	1.15571(54)	1.3
	16	1.16179(81)	0.5	1.15705(73)	0.4
	24	1.1607(13)	0.4	1.1576(12)	0.3
	32	1.1593(19)	0.3	1.1571(16)	0.4
	48	1.1616(34)	0.2	1.1596(28)	0.2
	64	1.1604(53)	0.2	1.1590(43)	0.2

by $\Delta_\epsilon = 3 - 1/\nu$, $\Delta_{\epsilon'} = 3 + \omega$, $\Delta_{\hat{\phi}} = (1 + \eta)/2$. We employ the recent MC results $\nu = 0.74817(20)$, $\omega = 0.755(5)$, $\eta = 0.03624(8)$ [70].

At the ordinary transition the $O(N)$ symmetry is unbroken, hence $a_1 = 0$ in Eqs. (S.4), (S.5) and (S.6). Thus, in the system of equations (S.5) and (S.6) there are 4 unknown parameters: 3 OPE coefficients p_ϵ , $p_{\epsilon'}$, $q_{\hat{\phi}}$ and $\Delta_{\hat{\phi}}$. In line with Ref. [40], a truncated solution can be searched by setting $M = 3$ in Eqs. (S.5)-(S.6). A nontrivial solution to the homogeneous linear set of equations (S.6) can exist only if the associated 3×3 matrix is singular [30]. To find a solution, we numerically search the minimum most singular value, as a function of the unknown dimension $\Delta_{\hat{\phi}}$. Within the numerical precision, we effectively find a zero of the most singular value, which corresponds to $\Delta_{\hat{\phi}} \simeq 1.172$. Given the general difficulty in estimating the systematic error due to the truncation [30, 40], we refrain here to quote an error bar. The calculation allows also to determine the boundary OPE coefficient $\mu_{\hat{\phi}}^2 = 0.867$. We have checked that, upon varying the input parameters within one error bar quoted in Ref. [70], the resulting value of $\Delta_{\hat{\phi}}$ changes on the fourth digit. Hence, the uncertainty on the input parameters is negligible with respect to the systematic error due to the truncation.

IX. FITS OF RG-INVARIANT OBSERVABLES

In Fig. S.1 we show the RG invariant (Z_a/Z_p) for $N = 2, 3, 4$. As expected, it exhibits a linear behavior in $1/L$, confirming the Ansatz of Eq. (8). In Table S.II we report fit results to Eq. (8), from which we have extracted the estimates given

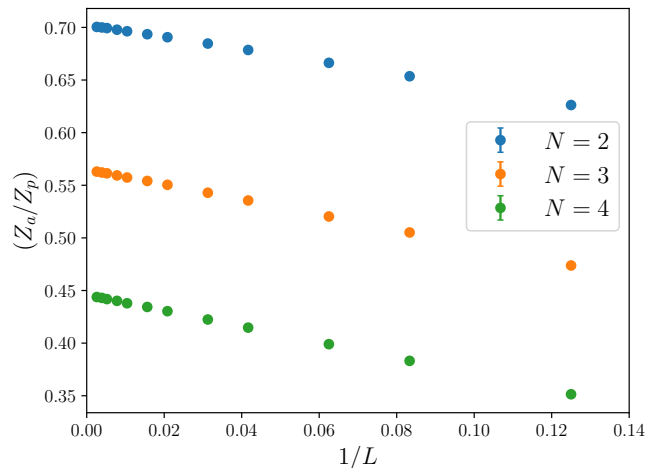


FIG. S.1. RG-invariant ratio (Z_a/Z_p) as a function of $1/L$

in Table III.

The helicity modulus Υ is computed by inserting a torsion of an angle θ along one of the two directions parallel to the surfaces. This can be obtained by replacing in the Hamiltonian (1)

$$\vec{\phi}_{\vec{x}} \cdot \vec{\phi}_{\vec{x}+\hat{e}_1} \rightarrow \vec{\phi}_{\vec{x}} R_{\alpha,\beta}(\theta) \vec{\phi}_{\vec{x}+\hat{e}_1}, \quad \vec{x} = (x_1 = x_{1,f}, x_2, x_3), \quad (\text{S.9})$$

where $R_{\alpha,\beta}(\theta)$ is a 2×2 matrix that rotates the α and β components of $\vec{\phi}$ by an angle θ . With a slight change of notation, in Eq. (S.9) $\vec{x} = (x_1, x_2, x_3)$ indicates the lattice site as a three-dimensional vector, and \hat{e}_1 is the unit vector in the

TABLE S.II. Fits of the RG invariant (Z_a/Z_p) to Eq. (8), for $N = 2, 3, 4$, and as a function of the minimum lattice size L_{\min} taken into account.

N	L_{\min}	$(Z_a/Z_p)^*$	$\chi^2/\text{d.o.f.}$
2	8	0.702585(30)	74.7
	12	0.702325(32)	11.9
	16	0.702242(33)	5.8
	24	0.702176(37)	3.9
	32	0.702129(40)	3.2
	48	0.702072(49)	3.1
	64	0.702051(59)	3.7
	96	0.701997(77)	4.6
	128	0.70184(10)	4.5
192	0.70156(14)	0.7	
3	8	0.565410(45)	21.1
	12	0.565101(50)	4.3
	16	0.565022(54)	2.9
	24	0.564910(62)	1.2
	32	0.564877(69)	1.2
	48	0.564800(82)	0.9
	64	0.564804(98)	1.1
	96	0.56494(13)	0.8
	128	0.56485(16)	0.6
192	0.56460(28)	0.0	
4	8	0.446078(51)	2.6
	12	0.445969(59)	1.4
	16	0.445901(67)	1.0
	24	0.445862(78)	1.0
	32	0.445856(92)	1.2
	48	0.44577(11)	1.1
	64	0.44572(13)	1.2
	96	0.44589(18)	1.0
	128	0.44566(25)	0.5
192	0.44589(42)	0.6	

1-direction; within this notation, the surfaces are located at $x_3 = 1, L$. The torsion of Eq. (S.9) is placed on a “defect” plane $x_1 = x_f$ and acts on the direction 1. With a suitable change of variables, it is possible to “smear out” the torsion over the entire length orthogonal to the defect plane [57]. The helicity modulus Υ is defined as [97]

$$\Upsilon \equiv \frac{L}{S} \frac{\partial^2 F(\theta)}{\partial \theta^2} \Big|_{\theta=0}, \quad (\text{S.10})$$

where $S = L_{\parallel}^2 = L^2$ is the area of the surfaces, and F is the free energy in units of $k_B T$.

As in Ref. [57], an improved estimator for Υ can be obtained by averaging over the $N(N-1)/2$ pairs of components (α, β) where the torsion is applied, as well as on the two possible lateral directions where the torsion is inserted.

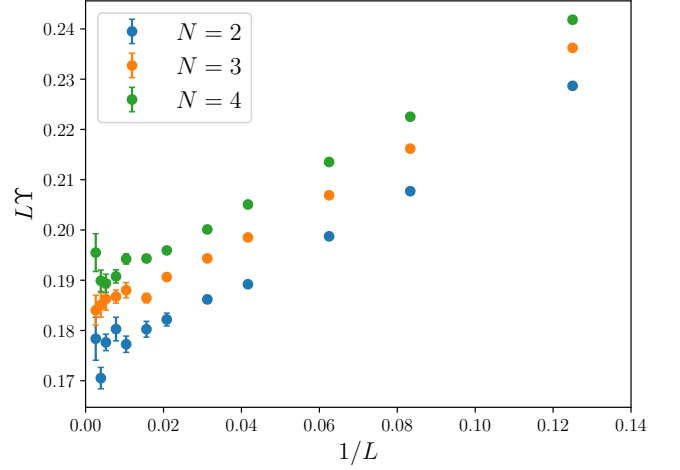


FIG. S.2. RG invariant $L\Upsilon$ as a function of $1/L$

TABLE S.III. Fits of the RG invariant $L\Upsilon$ to Eq. (8), for $N = 2, 3, 4$, and as a function of the minimum lattice size L_{\min} taken into account. Here we consider only MC data for $L \leq L_{\max} = 48$ (see text).

N	L_{\min}	$(L\Upsilon)^*$	$\chi^2/\text{d.o.f.}$
2	8	0.16922(43)	7.7
	12	0.17222(72)	1.1
	16	0.1727(10)	1.5
	24	0.1759(22)	0.2
3	8	0.17861(26)	13.8
	12	0.18103(43)	1.9
	16	0.18207(63)	0.2
	24	0.1825(12)	0.1
4	8	0.18564(18)	10.1
	12	0.18704(29)	0.9
	16	0.18720(43)	1.2
	24	0.18637(82)	1.0

One obtains the expression:

$$\begin{aligned} \Upsilon &= \frac{1}{2L^3} \left[\frac{2}{N} \langle E \rangle - \sum_{\hat{e}=\hat{e}_1, \hat{e}_2} \frac{2}{N(N-1)} \sum_{\alpha < \beta} \langle (T_{\hat{e}}^{(\alpha, \beta)})^2 \rangle \right], \\ E &\equiv \beta \sum_{\substack{\vec{x} \in \text{bulk} \\ \hat{e}=\hat{e}_1, \hat{e}_2}} \vec{\phi}_{\vec{x}} \cdot \vec{\phi}_{\vec{x}+\hat{e}} + \beta_s \sum_{\substack{\vec{x} \in \text{surface} \\ \hat{e}=\hat{e}_1, \hat{e}_2}} \vec{\phi}_{\vec{x}} \cdot \vec{\phi}_{\vec{x}+\hat{e}} \\ T_{\hat{e}}^{(\alpha, \beta)} &\equiv \beta \sum_{\vec{x} \in \text{bulk}} \left(\phi_{\vec{x}}^{(\alpha)} \phi_{\vec{x}+\hat{e}}^{(\beta)} - \phi_{\vec{x}}^{(\beta)} \phi_{\vec{x}+\hat{e}}^{(\alpha)} \right) \\ &\quad + \beta_s \sum_{\vec{x} \in \text{surface}} \left(\phi_{\vec{x}}^{(\alpha)} \phi_{\vec{x}+\hat{e}}^{(\beta)} - \phi_{\vec{x}}^{(\beta)} \phi_{\vec{x}+\hat{e}}^{(\alpha)} \right), \end{aligned} \quad (\text{S.11})$$

which is a generalization of the formula reported in Ref. [57].

In Fig. S.2 we show the RG-invariant combination $L\Upsilon$ as a function of $1/L$. While we observe a linear behavior in $1/L$ for $L \lesssim 64$, MC data for larger value of L are affected by considerable noise. Indeed, the formula for Υ (S.11) involves a delicate subtraction: the first term is the energy density, and

TABLE S.IV. Same as Table S.III for $L_{\max} = 64$.

N	L_{\min}	$(L\Upsilon)^*$	$\chi^2/\text{d.o.f.}$
2	8	0.16944(42)	7.1
	12	0.17242(67)	1.0
	16	0.17299(94)	1.1
	24	0.1754(17)	0.2
	32	0.1743(26)	0.0
3	8	0.17865(26)	11.1
	12	0.18086(41)	1.7
	16	0.18159(56)	1.1
	24	0.18130(96)	1.6
	32	0.1806(15)	3.0
4	8	0.18575(18)	9.3
	12	0.18713(28)	0.9
	16	0.18733(39)	1.0
	24	0.18693(67)	1.2
	32	0.1881(10)	0.3

converges to a finite positive value for $L \rightarrow \infty$. The second

term is manifestly positive and, subtracted to the energy term, must give a quantity $O(1/L)$, such that $L\Upsilon$ acquires a finite nontrivial value for $L \rightarrow \infty$. These considerations suggest a numerical instability of the sampled observable, which is clearly visible in Fig. S.2. Given these technical difficulties, we have decided to use only the MC data for $L \leq L_{\max} = 48, 64$ in the analysis. Corresponding fit results are reported in Tables S.III, S.IV. From the fits obtained with $L_{\max} = 48$, judging conservatively the stability of the results and the value of $\chi^2/\text{d.o.f.}$, we can estimate $(L\Upsilon)^* = 0.176(2)$ for $N = 2$, $(L\Upsilon)^* = 0.1821(6)$ for $N = 3$, and $(L\Upsilon)^* = 0.1864(9)$ for $N = 4$. Using the fits for $L_{\max} = 64$, we obtain $(L\Upsilon)^* = 0.174(3)$ for $N = 2$, and $(L\Upsilon)^* = 0.1873(4)$ for $N = 4$; for $N = 3$ the fit with $L_{\min} = 16$ gives $(L\Upsilon)^* = 0.18159(56)$, although with a slightly large $\chi^2/\text{d.o.f.} = 1.1$, while other fits have a large $\chi^2/\text{d.o.f.}$. The final values quoted in Table III are an average of the estimates found with $L_{\max} = 48, 64$, with an uncertainty fixed so as to have fully compatibility to such estimates within one error bar.